Remarkable Blue Shifts of C−H and N−H Stretching Frequencies in the Interaction of Monosubstituted Formaldehyde and Thioformaldehyde with Nitrosyl Hydride

Nguyen Tien Trung,[†,§] Tran Thanh Hue,[‡] and Minh Tho Nguyen*[,§]

Faculty of Chemistry, Quy Nhon University, Quy Nhon, Vietnam, Faculty of Chemistry and Center for Computational Science, Hanoi National University of Education, Hanoi, Vietnam, and Department of Chemistry and LMCC-Mathematical Modeling and Computational Science Center, Katholieke Universiteit Leuven, B-3001 Leuven, Belgium

Received: December 9, 2008; Revised Manuscript Received: January 24, 2009

Weak interactions of monosubstituted formaldehydes and thioformaldehydes with nitrosyl hydride were investigated by using ab initio MO calculations at the MP2/aug-cc-pVTZ level. Thirty two equilibrium structures having different complex forms were located on the corresponding potential energy surfaces (all having C_s symmetry). Obtained binding energies, which include both ZPE and BSSE corrections, range from 7 to 14 kJ·mol^{-1} and 6 to 12 kJ·mol^{-1} for complexes of substituted formaldehydes and thioformaldehydes, respectively. In each geometrical structure, the (XCHO,HNO) complex is consistently more stable than the (XCHS,HNO) complex. The H-bond strength significantly increases when one H atom is replaced by a methyl group in both formaldehyde and thioformaldehyde. When replacing H by a halogen atom, the binding energy tends to decrease. It is remarkable that all the C−H and N−H bonds are shortened upon complexation, resulting in an increase of their stretching frequencies. Furthermore, the blue shifts are consistently observed for the interacting N−H bonds in N−H···X, Z, with X = F, Cl, Br, and Z = O, S; such contraction of a covalent N−H bond is extremely rare. In addition, the N−H bond length contraction and its frequency blue shift in the N−H···S complex have been revealed for the first time.

1. Introduction

Noncovalent interactions play an important role in many fields of chemistry and biochemistry as they determine the structures and properties of liquids, molecular crystals, and biological molecules.[1−4] Among possible noncovalent interactions, the hydrogen bond is of particular significance.[5−8] Owing to its crucial importance, a large number of studies on the hydrogen bond phenomenon have been reported over the years including both theoretical calculations and experimental results.[9−15] A hydrogen bond is of the A−H···B type, where A is an electronegative atom and B is either an electronegative atom having one or more lone pairs or a region with excess electron density such as a negative charge or an aromatic π-system.[16,17] Normally, there is an elongation of the A−H bond length as compared to the respective monomer upon complexation. This corresponds to a decrease in its stretching frequency and an increase in the associated infrared intensity. This type of hydrogen bond is usually called a "normal hydrogen bond", or "standard hydrogen bond", or "classical hydrogen bond". There exists another type of hydrogen bond that results in a contraction of the A−H bond and a blue shift of the stretching frequency. In general, a decrease of the infrared intensity is induced when the A−H bond is contracted. Initially, this was called an "anti-hydrogen bond",[18] which was, however, inappropriate because it evoked an idea that it is not a hydrogen bond. More recently, it was renamed as an "improper blue-shifting hydrogen bond"[19] or a "blue-shifted hydrogen bond".[20] While the characteristics of the normal hydrogen bond are well understood, the origin of the blue-shifting hydrogen bond remains a matter of debate. Although there are many different opinions about the origin of blue-shifting and red-shifting in hydrogen bonds, it has been proposed that there is actually no unambiguous distinction between both types of hydrogen bond.[21,22] Several hypotheses and models have in fact been proposed to explain the differences between the blue shift and red shift of the stretching frequency in the A−H bonds following complexation.[12−15,23−27] However, no general explanation has been put forward for the origin of all H-bonded complexes that possess the blue-shifting phenomenon.

Numerous studies on blue-shifting hydrogen bonds have concentrated on C−H as the proton donor, whereas this phenomenon involving a N−H bond is less known. The stretching vibrational frequency of an N−H bond is usually expected to shift to the red upon complexation due to its large polarization. There have, however, been a few exceptions observed for the contraction and blue shift of a N−H bond in the type N−H···O.[28−34] Besides, bond length shortening and frequency blue shift of the N−H bond are also observed in some dihydrogen bond complexes.[35−37] To the best of our knowledge, only a few studies have recently been devoted to the existence of blue-shifting N−H···X bonds with X = halogen atoms.[21,29,32−34,38] The N−H blue shift in N−H···S complexes has not been reported in the literature yet. It is also remarkable that the HNO molecule containing a N−H bond can act as either a proton donor or a proton acceptor, which is important in many processes such as pollution formation, energy release in propellants, and fuel combustion.[39] A few earlier studies reported on the formation of blue-shifting complexes of HNO with carbonyls. Yang and co-workers[31] showed a blue shift of both the C−H and N−H bonds in $CH_3CHO\cdots HNO$. Blue-shifted C−H bonds were also detected in the complexes between simple carbonyls such as HCHO, FCHO, and HNO, and between HCHO and HF.[40−42]

* E-mail: trung.nguyen@chem.kuleuven.be; minh.nguyen@chem.kuleuven.be.
† Quy Nhon University.
§ Katholieke Universiteit Leuven.
‡ Hanoi National University of Education.

10.1021/jp810826z CCC: $40.75
Published on Web 03/03/2009

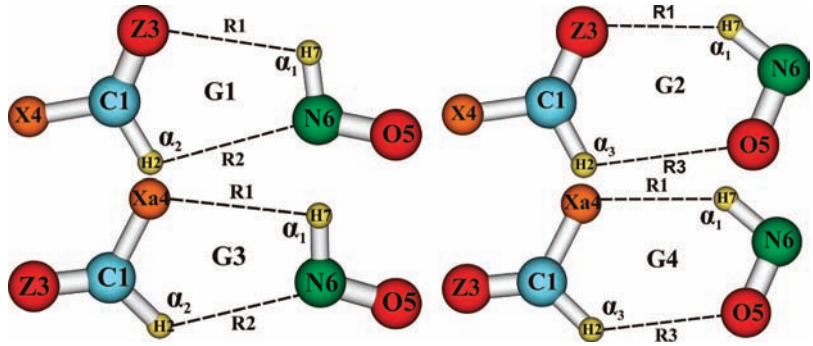

Figure 1. The optimized geometry of complexes pairing XCHZ with HNO (X = CH_3, H, F, Cl, Br; Xa = F, Cl, Br; Z = O, S).

TABLE 1: Changes of the C1−H2 and N6−H7 Bond Lengths upon Complexation (Δr, in 10^{-3} Å)

		XCHO···HNO[a]				XCHS···HNO[a]			
		G1	**G2**	**G3**	**G4**	**G1**	**G2**	**G3**	**G4**
X = F	Δr(C1−H2)	−1.1	−1.6	−1.2	−1.4	−0.6	−1.3	−1.0	−1.4
	Δr(N6−H7)	−3.3	−4.2	−1.7	−2.9	−2.5	−2.1	−1.7	−2.8
X = Cl	Δr(C1−H2)	−1.1	−1.6	−1.1	−1.7	−0.4	−1.1	−0.5	−1.2
	Δr(N6−H7)	−3.1	−3.9	−1.6	−1.8	−2.5	−2.2	−1.3	−1.5
X = Br	Δr(C1−H2)	−1.2	−1.7	−0.8	−1.7	−0.4	−1.1	−0.3	−1.1
	Δr(N6−H7)	−2.9	−3.7	−1.9	−1.4	−2.5	−2.1	−13	−0.9
X = H	Δr(C1−H2)	−2.2	−3.4			−0.7	−1.7		
	Δr(N6−H7)	−5.1	−5.1			−2.9	−2.7		
X = CH_3	Δr(C1−H2)	−2.3	−4.0			−0.9	−2.1		
	Δr(N6−H7)	−5.3	−5.5			−2.8	−2.7		

[a] See Figure 1 for definition of the complex structures **G1**, **G2**, **G3**, and **G4**.

Considering that a systematic examination of complexes formed from substituted carbonyls with nitrosyl hydride could shed light on the general behavior, we set out to theoretically consider in the present work the molecular interaction between XCHZ and HNO in which X = CH_3, H, F, Cl, and Br, and Z = O and S, at a high level of theory. Our main goal is to obtain some features for a better understanding of the origin of the blue-shifting hydrogen bond, not only for the C−H bonds, but also for the N−H bonds in the types N−H···X, Z.

2. Computational Methods

In the present work, we performed a detailed examination of interaction energies, electronic structure, stretching frequency, charge distribution, orbital occupation, and a topological analysis. Geometry optimization for all the structures including monomers and complexes was carried out by using the second-order perturbation theory (MP2) in conjunction with the large correlation consistent basis set, aug-cc-pVTZ,[43] which include both s,p-diffuse and p,d,f-polarization functions. This level of theory has proved to be quite good in evaluating geometric and energetic parameters for H-bonded complexes.[44−46] The geometries were fully optimized without symmetry constraint. Harmonic vibrational frequencies were subsequently performed at the same level to identify the true equilibrium structures, and to estimate their zero-point energies. The vibrational frequencies were retained unscaled. To avoid vibrational coupling between the CH_2 stretching modes in HCHO and HCHS, harmonic frequencies were calculated in the DCHO and DCHS isotopomers for both monomers and complexes. Interaction energies were obtained as the difference between the energies of the complexes and the respective monomers, and corrected for basis set superposition errors (BSSE) by using the counterpoise procedure.[47] Geometry optimizations were performed with the Gaussian 03 suite of programs.[48] Topological properties of electron density were analyzed by using the AIM 2000[49] software for the Atoms-in-Molecules (AIM) theory.[50,51] Natural bond orbital (NBO) analysis was also performed with use of of the GenNBO 5.0G program at the same MP2/aug-cc-pVTZ level.[52] Cartesian coordinates of complexes and change in geometrical parameters are given in the Supporting Information.

3. Results and Discussion

3.1. Geometries, Stretching Frequencies, and Infrared Intensities. Our search for minimum energy structures on relevant potential energy surfaces of substituted formaldehyde and thioformaldehyde XCHZ (X = H, CH_3, F, Cl, Br; Z = O, S) with nitrosyl hydride HNO led to 32 different structures, in which there are 8 structures for each of the substrates X = F, Cl, and Br, and four structures for each of X = H and CH_3. The shape of the optimized structures of these dimers is displayed in Figure 1, while the changes of selected geometrical parameters in complexes predicted at the MP2/aug-cc-pVTZ level are gathered in Table 1 (the full table of distances is given in the Supporting Information). The four different structures are referred to hereafter as **G1**, **G2**, **G3**, and **G4**. Calculated C−H bond lengths and proton affinities at the O and S sites in the isolated monomers considered are very close to the experimental results as collected in Table 2. The obtained results indicate again that the MP2/aug-cc-pVTZ level is reasonably reliable for the problems under consideration. All examined complexes were optimized to cyclic C_s structures. Calculated results (given in Table S1 in the SI) show that all intermolecular contacts denoted as R1, R2, and R3 are shorter than the sum of van der Waals radii. In addition, the corresponding hydrogen bond angles labeled α1, α2, and α3 are larger than 90°, which is beneath the limitation for formation of hydrogen bond. These angles are indeed in the range of 96.6−149.9°, 106.8−133.9°, and 111.0−137.9° for α1, α2, and α3, respectively. Therefore, the intermolecular contact in all minima can roughly be categorized as a hydrogen bond. The origin of these bonds will

TABLE 2: Calculated C−H Bond Length (*r*, in Å) and Proton Affinity (PA, in kJ·mol^{-1}) at O and S Sites in Isolated Monomers at the MP2/aug-cc-pVTZ Level

	CH_3CHO	HCHO	FCHO	ClCHO	BrCHO	CH_3CHS	HCHS	FCHS	ClCHS	BrCHS
r(C1−H2)	1.1058	1.1006	1.0904	1.0926	1.0934	1.0909	1.0868	1.0862	1.0854	1.0853
exptl[a]	1.1140[a]	1.1110[a]				1.0890[a]	1.0870[a]			
PA[b]	728.9	684.9	615.5	649.4	657.3	769.4	726.3	682.8	715.0	723.8
exptl[a]	736.4[a]	683.2[a]					730.5[a]			

[a] Experimental data taken from NIST webpage http://webbook.nist.gov/chemistry. [b] Calculated proton affinities include ZPE corrections at the same level.

TABLE 3: Changes of Stretching Frequency (Δ*v*, in cm^{-1}) and IR Intensity (Δ*I*, in km·mol^{-1})

		XCHO···HNO				XCHS···HNO			
		G1	**G2**	**G3**	**G4**	**G1**	**G2**	**G3**	**G4**
X = F	Δ*v*(C1−H2)	18	26	20	24	13	23	17	22
	Δ*v*(N6−H7)	62	89	35	65	47	49	34	61
	Δ*I*(C1−H2)	−11	−12	−15	−14	−2	−2	−3	−4
	Δ*I*(N6−H7)	−55	−76	0	−61	−47	−76	−39	−58
X = Cl	Δ*v*(C1−H2)	21	27	21	31	11	21	13	23
	Δ*v*(N6−H7)	58	83	34	45	48	49	29	39
	Δ*I*(C1−H2)	−12	−13	−10	−11	9	6	16	9
	Δ*I*(N6−H7)	−52	−74	−43	−64	−50	−75	−40	−57
X = Br	Δ*v*(C1−H2)	22	28	18	31	11	21	10	21
	Δ*v*(N6−H7)	55	80	38	41	47	48	29	33
	Δ*I*(C1−H2)	−12	−12	−5	−8	14	11	21	13
	Δ*I*(N6−H7)	−51	−73	−48	−70	−51	−76	−43	−64
X = H	Δ*v*(C1−H2)	34	48			15	28		
	Δ*v*(N6−H7)	93	102			58	55		
	Δ*I*(C1−H2)	−39	−43			−8	−7		
	Δ*I*(N6−H7)	−77	−76			−72	−76		
X = CH_3	Δ*v*(C1−H2)	34	53			17	32		
	Δ*v*(N6−H7)	104	106			59	56		
	Δ*I*(C1−H2)	−47	−57			−14	−13		
	Δ*I*(N6−H7)	−89	−66			−83	−73		

be explored in a following section. Along with the changes in bond lengths, the changes of stretching frequencies and infrared intensities of both C1−H2 and N6−H7 bonds are collected in Table 3. Interestingly, the changes in bond length due to complex formation, described by the parameters Δ*r*(C1−H2) and Δ*r*(N6−H7), are consistently negative, indicating that complex formation leads to contraction of these bonds, as compared to the isolated monomers. The contraction lies in the range of 0.0003−0.0040 Å for the C1−H2 bond lengths and of 0.0009−0.0055 Å for the N6−H7 bond lengths. While the smallest decrement of the C1−H2 bond is predicted for **G3** of BrCHS···HNO, the largest is for **G2** of CH_3CHO···HNO. It is remarkable that the largest contraction is also obtained for the N6−H7 bond in CH_3CHO···HNO (**G2**), and the smallest in **G4** of BrCHS···HNO.

Accompanying the contraction of C1−H2 and N6−H7 bonds, different changes also occurred in each of the geometries examined, when the complexes are formed. Thus the H-bonded C1−X4 bonds are elongated, whereas the nonbonded C1−X4 bonds are shortened in all XCHZ···HNO complex structures compared to the respective monomers. Similarly, an elongation of H-bonded C1═Z3 bonds in **G1** and **G2** for complexes XCHZ···HNO is also observed. The nonbonded C1═Z3 bonds are contracted in **G3** and **G4** as shown in the full Table S1 in the SI. In other words, the C1═Z3 and C1−X4 bonds involved in a hydrogen bond are elongated upon complexation, and vice versa. All of the N6—O5 bonds are moderately elongated, except for a very marginal contraction predicted in **G3** of XCHZ···HNO (X = F, Cl and Br).

Increase in stretching frequencies, which corresponds to contraction of the C1−H2 and N6−H7 bond lengths, is also observed in all complexes. Indeed, results summarized in Table 3 indicate that the *v*(C1−H2) stretching frequencies are shifted to blue by 10−53 cm^{-1}, and the *v*(N6−H7) stretching frequencies are shifted by 29−106 cm^{-1}. A blue-shifting A−H···B hydrogen bond usually shortens the A−H bond and decreases the A−H stretching intensity, and vice versa. This tendency is equally predicted for the N6−H7 bonds in all complexes examined. The absolute values for IR intensities decrease considerably, up to 89 km·mol^{-1}. A similar trend is also found for C1−H2 bonds in some of the structures **G1**, **G2**, **G3**, and **G4** of the interaction between XCHZ and HNO. Such decrease is in the range of 2−57 km·mol^{-1}. However, a slight increase of 6−21 km·mol^{-1} in IR intensity of C1−H2 bonds is revealed in some structures of the complexes XCHS···HNO (X = Cl, Br), in spite of a bond length shortening and an effective increase of their stretching frequencies. Our results obtained in this work and reported in a previous publication[38] and the data reported by other authors[53] demonstrated that IR intensity can actually be increased even when the bond length is contracted following complexation, along with an increase in its stretching frequency. The change of IR intensity depends on the inherent property of the monomer rather than the dimer. Contractions of both C1−H2 and N6−H7 bonds and increases in their stretching frequencies indicate that the corresponding intermolecular contacts can be classified as blue-shifted hydrogen bonds.

The magnitude of contraction and frequency blue shift of the C1−H2 bond in some complexes is close to, or somewhat larger than, the values reported in some previous literature.[31,40] Ying and co-workers[31] predicted a contraction of the C−H bond length by 0.0010 Å in FCHO···HNO and 0.0034 Å in HCHO···HNO, leading to an increase in stretching frequency by 19 cm^{-1} for the former and 21 (symmetric mode) and 38 cm^{-1} (asymmetric mode) for the latter, calculated at the MP2/

6-311++G(2d,2p) level of theory. Furthermore, Yang and coworkers[40] reported a contraction of 0.0031 Å and a blue shift of 42 cm^{-1} for the C−H bond in $CH_3CHO\cdots HNO$ computed at the MP2/6-311++G(d,p) level. The results obtained for structure **G2** of $CH_3CHO\cdots HNO$ in this work, which corresponds to the geometry mentioned in ref 40, amount to 0.004 Å and 53 cm^{-1}.

To further understand the changes observed for C1−H2 bond lengths upon complexation, let us consider their capacity of polarization in the monomers. When replacing an H atom of formaldehyde by a methyl CH_3 or a halogen X, an increment of the C−H bond length occurs in going from F via Cl to Br, and from H to CH_3, as gathered in Table 2. However, a slight increase in C−H bond length is predicted in the sequence from Br to Cl to F to H and finally to CH_3 in substituted thioformaldehydes. Generally, the C−H bond length is getting shorter in the isolated XCHS monomers than in the relevant XCHO ones. This implies that a polarization of the C−H bond is expected to be larger in XCHS than in XCHO. In this regard, experimental deprotonation enthalpies of the monomers can be used to quantitatively prove the weaker polarity of C−H bonds in XCHO. However, there are only a few available data reported in the popular webpage of National Institute of Standards and Technology (NIST).[54] For instance, the deprotonation enthalpy is reported as 1456 ± 14 kJ·mol^{-1} for CH_3CHS and 1636 ± 9 kJ·mol^{-1} for CH_3CHO. These indicate that the capacity of polarization of a C−H bond is larger for the former than for the latter. Hence, the longer the length of the bond, the smaller the capacity of polarization. It can thus be expected that a shortening of the C−H bond length and a blue shift in its frequency are larger for XCHO than for XCHS, with the same proton acceptor in similar geometric structure. Obtained results in Tables 1 and 3 lend support for such a view. Therefore, contraction and blue shift of a C−H bond apparently depend on properties of the isolated monomer, in particular on its polarity. The changes in C1−H2 bond lengths and their stretching frequencies are marginally sensitive to the nature of the halogen in progressing from F via Cl to Br (cf. Tables 1 and 3).

As mentioned in the Introduction, contraction of a covalent N−H bond has seldom been detected due to its polarity. In a few remarkable cases, N−H blue shifts with different magnitudes have recently been predicted for both dihydrogen and hydrogen bond complexes.[30−38] For a dihydrogen bond such as in the complex pairing BH_3NH_3 with HNO,[35] the N−H frequency undergoes a blue shift of 128 cm^{-1}. A moderate N−H blue shift has been also obtained in the complexes between YH_2NH_2 (Y = B, Al) and HNZ (Z = O, S).[36] A significantly strong N−H blue shift has been found in some H-bonded complexes of CH_3X with HNO, HNO with HNO, HNO with $HFSO_2$, and HOX with HNO, which amounts up to ∼100 cm^{-1}.[30,32−34] A comparable frequency blue shift of ca. 22−106 cm^{-1} for the N6−H7 bond in the type N6−H7···X, Z (Z = O, S; X = halogens) is also observed in all complexes considered here, along with a contraction of N6−H7 bond length. The largest blue shift is observed for **G2** of $CH_3CHO\cdots HNO$, and the smallest one for **G3** of $BrCHS\cdots HNO$. The magnitudes of the decrease in the N6−H7 bond length and increase in its stretching frequency are also in line with those previously reported as mentioned above. There is only a small difference in the magnitude of the N−H stretching frequency, which is 126 cm^{-1} in ref 31 and 106 cm^{-1} in this work for the pair of CH_3CHO with HNO (**G2**). The difference is no doubt due to the use of a larger basis set in the present work. The blue shift associated with an N−H bond is significantly larger than that with a C−H bond. N−H bond contraction and blue shift were rarely evaluated because of the high acidity of the N−H bond. Combining our obtained results[36,38] with the literature data[28−35,37,40] we would suggest that the contraction and blue shift of a N−H bond form a peculiar behavior of the HNO molecule. The blue shift of both the C−H and N−H frequencies are consistent with the contraction noted above for their equilibrium bond lengths.

Highly linear correlations between the changes in C1−H2 and N6−H7 bond lengths and their respective stretching frequencies can be obtained as expressed in eqs 1 and 2, and plotted in Figure 2:

$$\Delta\upsilon(\text{C}-\text{H})\ (\text{cm}^{-1}) = -12043\Delta r(\text{C}-\text{H})\ (\text{Å}) + 7.0408 \quad (r = 0.99) \quad (1)$$

$$\Delta\upsilon(\text{N}-\text{H})\ (\text{cm}^{-1}) = -17758\Delta\upsilon(\text{N}-\text{H})\ (\text{Å}) + 8.4094 \quad (r = 0.98) \quad (2)$$

The slope of eq 2 is larger than that of eq 1, indicating a greater sensitivity of the υ(N6−H7) stretching modes to variations of the corresponding bond length. This finding is consistent with that reported in ref 38.

It is perhaps remarkable that the N−H contraction and blue shift are larger in the N−H···O complexes than in the N−H···S counterparts in all the **G1** and **G2** structures shown in Tables 1 and 3. For **G3** and **G4** structures of N−H···X (X = F, Cl, Br), N−H bond length contraction and increase in its frequency are also larger for XCHO···HNO than for XCHS···HNO. In general, these parameters tend to decrease in going from F via Cl to Br for each type of structure of XCHZ···HNO, even though the respective deviation is not large.

In summary, the length contraction and the frequency blue shift of an H-bonded N−H bond are larger for N−H···O than for N−H···S complexes. This can be understood by considering the difference in gas phase basicity at the O and S sites. More quantitatively, calculated results of proton affinities recorded in Table 2, which are in good agreement with available

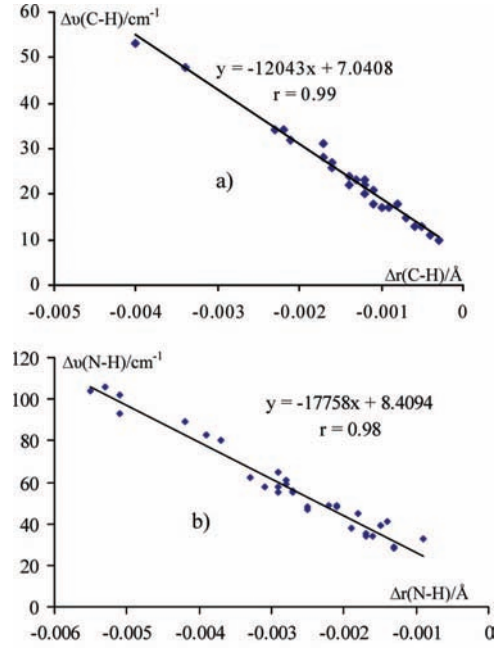

Figure 2. Linear correlation between (a) $\Delta\upsilon$(C−H) and Δr(C−H) and (b) $\Delta\upsilon$(N−H) and Δr(N−H).

TABLE 4: Interaction Energy with ZPE but without BSSE (E^0) and with Both ZPE and BSSE (E^1) Corrections (in kJ·mol^{-1})

		XCHO···HNO				XCHS···HNO			
		G1	**G2**	**G3**	**G4**	**G1**	**G2**	**G3**	**G4**
X = F	E^0	−10.8	−12.7	−8.6	−8.9	−10.8	−12.3	−8.5	−8.6
	E^1	−9.0	−10.5	−6.8	−6.6	−8.7	−9.5	−6.6	−6.4
	BSSE	1.8	2.2	1.8	2.3	2.2	2.7	1.9	2.3
X = Cl	E^0	−11.0	−12.7	−11.0	−11.3	−11.4	−12.9	−10.0	−10.2
	E^1	−9.0	−10.3	−8.8	−8.7	−9.0	−9.9	−7.8	−7.7
	BSSE	2.0	2.4	2.2	2.6	2.4	2.9	2.2	2.6
X = Br	E^0	−11.6	−13.3	−13.5	−14.6	−12.1	−13.5	−12.0	−12.9
	E^1	−8.9	−10.1	−9.9	−9.5	−8.9	−9.9	−8.4	−8.0
	BSSE	2.8	3.2	3.7	5.1	3.2	3.7	3.6	5.0
X = H	E^0	−11.0	−13.4			−10.5	−12.4		
	E^1	−9.2	−11.3			−8.3	−9.9		
	BSSE	1.7	2.1			2.2	2.5		
X = CH_3	E^0	−13.2	−15.9			−12.7	−14.9		
	E^1	−11.2	−13.6			−10.2	−12.1		
	BSSE	1.9	2.3			2.5	2.8		

experimental values, indicate that the gas phase basicity is larger on the S atom than on the O atom in the respective monomer.

3.2. Interaction Energy. Interaction energies of the 32 complexes considered were calculated at the equilibrium geometries by the MP2/aug-cc-pVTZ level, and the results are collected in Table 4. The interaction energies were corrected for ZPE (E^0) and for both ZPE and BSSE (E^1). All evaluated interaction energies are significantly negative. Binding energies obtained in this work are in a good agreement with those previously reported.[31,40] In particular, our values for binding energies amount to 9.2, 9.0, and 11.2 kJ·mol^{-1} for HCHO···HNO (**G1**), FCHO···HNO (**G1**), and CH_3CHO···HNO (**G1**), respectively. These are comparable to the values of 9.2 and 8.9 kJ·mol^{-1} for HCHO···HNO and FCHO···HNO determined by using the G3B3 level in ref 40 and 10.0 kJ·mol^{-1} for CH_3CHO···HNO at the MP2/6-311++G(d,p) level in ref 31. The calculated binding energies lie in the range of 6−14 kJ·mol^{-1} including both ZPE and BSSE corrections (8−16 kJ·mol^{-1} only with ZPE). The most stable complex corresponds to the **G2** geometry (13.6 kJ·mol^{-1}) of CH_3CHO···HNO, and the least stable the **G4** of FCHS···HNO (6.4 kJ·mol^{-1}).

Influence of substitution (X = CH_3, H, F, Cl, Br) on interaction energies in XCHZ···HNO was examined in detail. For **G1** and **G2** structures in XCHO···HNO, it is found that the strength of the complexes generally decreases in the following ordering: CH_3 > H > F ≥ Cl >Br. However, this ordering is different for **G1** and **G2** in XCHS···HNO. For **G1**, binding energies tend to decrease in going from CH_3 via Cl via Br via F to H, while such a sequence is not observed for **G2** (CH_3 > Cl > H > Br > F). Furthermore, the **G2** geometries are found to be more stable than the **G1** ones in each type of XCHO···HNO and XCHS···HNO complexes. Results for the shorter R1, R2, and R3 intermolecular distances in **G2** compared to those in **G1** are shown in the full Table S1 in the SI. The difference in intermolecular distances can be accounted for by the various polarities of the C1−H2 bond in the isolated monomers as discussed above. With a larger C−H polarity in the XCHS, the (R2, R3) intermolecular distance of the contacts C1−H2···O5,N6 in XCHS···HNO is indeed shorter than that in XCHO···HNO when the H-bonded complex is formed (as listed in Table S1 in the SI). This can be expected to result in stronger XCHS···HNO complexes. However, the strength of **G1** and **G2** in XCHO···HNO turns out to be larger than that in XCHS···HNO, respectively. This clearly indicates that these complexes are primarily stabilized by the intermolecular contacts Z3···H7−N6.

For **G3** and **G4** complexes (Table 4), the strength of H-bonded complexes is found to increase in the ordering *F* < Cl < Br either with BSSE or without BSSE correction in all complexes considered. This ordering is consistent with a higher acidity of the C−H bond in the isolated XCHS monomers and is in contrast to that in the isolated XCHO monomers, in going from F via Cl to Br. It indicates that the strength of **G3** and **G4** complexes of interaction between XCHO and HNO is mainly determined by the X4···H7−N6 (X = halogens) intermolecular contacts instead of the C1−H2···O5,N6 ones. The strength of **G4** is expected to be larger than that of **G3**, because the resulting (R1, R2, and R3) intermolecular distances are uniformly shorter in **G4**. It is surprising that a **G4** geometry is more stable than a **G3** geometry without BSSE correction, while a reversed direction is predicted when BSSE correction is taken into account. Generally this deviation is relatively small, only ca. <0.5 kJ·mol^{-1}. It can be understood that the BSSE contribution to the interaction energy is significantly larger in **G4** than in **G3** as shown in Table 4. The results also point out that **G3** and **G4** of XCHO···HNO are marginally more stable than XCHS···HNO. The CH_3CHO···HNO complex is found to be the most stable in all complexes considered. The effect of the halogen atom on binding energies is rather small, with the difference in the binding energies being ca. 0.5 kJ·mol^{-1} in each geometric type. It is worth mentioning that the strength of H-bonded complexes significantly increases when a hydrogen atom is replaced by a methyl group on both formaldehyde and thioformaldehyde. The increase amounts to ca. 2.0 kJ·mol^{-1} for both substituted formaldehydes and thioformaldehydes (with both BSSE and ZPE corrections). Reversely, when substituting hydrogen by a halogen, the binding energy tends to decrease as shown in Table 4.

3.3. An AIM Analysis. In an attempt to probe the consistency and understand further the properties of hydrogen bonds in the complexes studied, we performed an "atoms-in-molecules" topological analysis (AIM). This methodology was used as a criterion for hydrogen bond formation and may provide an independent set of criteria to characterize the hydrogen bonds. Eight different criteria for hydrogen bond formation have been proposed by Popelier and Koch,[55] of which three are the most often applied. These can be summarized as follows: (1) a bond critical point (BCP) must be present (one of three λ_i eigenvalues of the Laplacian is positive and the other two negative, denoted as (3, −1)); (2) the electron density $\rho(r)$ at the BCP should be within the range 0.002−0.035 au; and (3) the Laplacian $\nabla^2(\rho)$ at the BCP should be between 0.02 and 0.15 au. The value of

TABLE 5: Topological Analysis of the XCHZ···HNO Complexes

		G1		G2		G3		G4	
complex structure		ρ (10^{-3} au)	∇^2 (10^{-2} au)	ρ (10^{-3} au)	∇^2 (10^{-2} au)	ρ (10^{-3} au)	∇^2 (10^{-2} au)	ρ (10^{-3} au)	∇^2 (10^{-2} au)
FCHO···HNO	O3,X4···H7	9	4	14	5	7	3	7	3
	O5,N6···H2	9	4	8	3	8	3	10	4
	RCP	8	4	7	3	6	3	10	4
ClCHO···HNO	O3,X4···H7	9	4	14	5	7	3	9	3
	O5,N6···H2	8	3	8	3	11	4	10	2
	RCP	7	4	7	3	6	3	9	2
BrCHO···HNO	O3,X4···H7	9	4	13	5	8	2	10	3
	O5,N6···H2	9	3	8	3	9	4	10	3
	RCP	7	4	8	3	6	3	8	3
HCHO···HNO	O3,X4···H7	12	5	11	4				
	O5,N6···H2	6	2	6	2				
	RCP	6	3	5	3				
CH_3CHO···HNO	O3,X4···H7	15	5	14	5				
	O5,N6···H2	5	2	10	2				
	RCP	5	3	7	3				
FCHS···HNO	S3,X4···H7	8	2	12	3	7	3	10	4
	O5,N6···H2	10	3	9	3	8	3	8	3
	RCP	6	3	5	2	6	3	5	2
ClCHS···HNO	S3,X4···H7	7	2	9	9	7	2	9	3
	O5,N6···H2	10	4	10	3	7	3	9	3
	RCP	6	3	5	2	6	3	5	2
BrCHS···HNO	S3,X4···H7			7	3			10	3
	O5,N6···H2	11	4	15	3	14	3	19	2
	RCP			6	2			6	3
HCHS···HNO	S3,X4···H7	11	3	11	3				
	O5,N6···H2	8	3	8	3				
	RCP	6	3	7	2				
CH_3CHS···HNO	S3,X4···H7	13	3	13	4				
	O5,N6···H2	8	3	8	3				
	RCP	7	3	6	2				

$\rho(r)$ can be used to measure the strength of a bond. In general, the larger the value of $\rho(r)$, the stronger the bond. The $\nabla^2(\rho)$ describes a bond characteristic: the bond is a covalent bond if $\nabla^2(\rho) < 0$, and if $\nabla^2(\rho) > 0$, the bond belongs to the ionic bond, van der Waals interaction, or hydrogen bond.

Electron densities and Laplacian values for critical points of intermolecular contacts in the complexes considered are collected in Table 5. Note that a critical point, denoted by (3, +1), is called a ring critical point (RCP) when one of three λ_i is negative and the other two are positive. There almost exist two BCPs and one RCP in each geometric structure, except for two geometries **G1** and **G3** of BrCHS···HNO. There is only one BCP of the intermolecular contact N6···H2−C1 in **G1** and in **G3** of BrCHS···HNO. Accordingly, no H-bond exists for the intermolecular contact S3···H7−N6 in **G1** and Br4···H7−N6 in **G3**. These intermolecular contacts can be approximated by the sum of van der Waals radii of both S and H atoms (3.05 Å), and both Br and H atoms (3.15 Å). Hence, the existence of considerably weak bonds of the intermolecular contacts S3···H7−N6 in **G1** and Br4···H7−N6 in **G3** of the complex BrCHS···HNO is mainly due to cohesive attractions between the S3 and H7 atoms on the one hand and Br4 and H7 atoms on the other hand. A similar observation was reported in ref 36.

As indicated in Table 5, electron densities are in the range of 0.007−0.015 au for the Z3,X4···H7−N6 contacts and of 0.005−0.019 au for the O5,N6···H2−C1 contacts. Their Laplacians also fall within criteria for H-bond formation. In particular, they are of 0.021−0.054 au for the Z3,X4···H7−N6 contacts and of 0.018−0.038 au for the O5,N6···H2−C1 contacts. Therefore, the intermolecular contacts presented above are considered as hydrogen bonds, and in this case as blue-shifted hydrogen bonds. Furthermore, the existence of ring structure is further characterized by a RCP in each **Gx** (**x** = 1, 2, 3, 4) structure. Of course, this remark does not include both **G1** and **G3** structures of the interaction between BrCHS and HNO.

3.4. An NBO Analysis. To gain a clearer view on the origin of the hydrogen bonds in the examined complexes, a NBO analysis has been performed at the MP2/aug-cc-pVTZ level and selected results are reported in Table 6. Clearly, there are different directions of electron density transfer (EDT) between XCHZ and HNO as a result of complex formation. The positive values of EDT mean that the electron density is transferred from HNO to XCHZ, and vice versa. As seen from Table 6, the transfer of electron density generally takes place from HNO to XCHZ, by an amount of 0.001−0.006 au. However, a reversed direction of moving the electron from XCHZ to HNO is observed for the dimers such as **G1** and **G2** of XCHZ···HNO (X = H, CH_3), **G2** of XCHS···HNO (X = F, Cl, Br), and **G4** of both BrCHO···HNO and BrCHS···HNO. Absolute EDT values in these complexes are in the range of 0.002−0.011 au. Most notably, the EDT reaches the zero value in **G2** of FCHO···HNO implying that the sum of transfer in electron density from FCHO to HNO is equal to that from HNO to FCHO. Particularly, these transfers are from n(O5) lone pairs to σ^*(C1−H2) antibonding orbital and from n(O3) lone pairs to σ^*(N6−H7) antibonding orbital. This charge-transfer interaction causes the strength of hydrogen bonds in all examined complexes.

Let us first examine in some detail the blue shifts of stretching frequencies of both the C1−H2 and N6−H7 bonds in all the considered complexes on the basis of NBO analysis. There is an increase of the s-character of C1(H2) atoms, by an amount of 0.3−1.8%. The significant increase of the C1(H2) s-character is predicted in **G3** and **G4** of XCHZ···HNO (X = F, Cl, Br

TABLE 6: NBO Analysis of the XCHZ···HNO Complexes (charges in 10^{-3} au)

parameter		$\Delta\sigma^*$(C1−H2)	$\Delta\sigma^*$(N6−H7)	Δ%sC1	Δ%N6	Δq(C1)	Δq(N6)	Δq(H2)	Δq(H7)	EDT
X = F, Z = O	G1	−1.7	−2.2	0.42	0.88	0	−25	16	22	3
	G2	−3.3	−3.9	0.40	1.34	6	−7	17	30	0
	G3	−0.7	−0.7	0.83	0.51	−9	−20	19	15	5
	G4	−1.4	−2.9	0.87	0.73	−8	3	19	18	3
X = Cl, Z = O	G1	−2.1	−2.0	0.42	0.83	−6	−25	16	21	4
	G2	−3.5	−3.4	0.32	1.27	−3	−6	16	28	1
	G3	−0.9	−0.1	1.49	0.59	7	−22	22	16	6
	G4	−2.5	−0.2	1.47	0.83	12	4	21	16	1
X = Br, Z = O	G1	−2.3	−1.8	0.46	0.80	−7	−25	16	20	4
	G2	−3.5	−3.1	0.31	1.23	−5	−4	16	27	1
	G3	−0.8	0.1	1.77	0.72	12	−25	24	18	6
	G4	−2.7	2.7	1.71	1.08	18	3	22	17	−2
X = H, Z = O	G1	−4.3	−3.2	0.40	1.38	2	−28	17	29	−2
	G2	−5.7	−3.5	0.49	1.77	8	−42	20	37	−5
X = CH_3, Z = O	G1	−4.8	−3.0	0.34	1.77	2	−32	16	35	−3
	G2	−6.7	−3.0	0.50	2.08	7	−22	22	42	−6
X = F, Z = S	G1	−0.8	−0.9	0.75	0.80	7	−23	16	18	3
	G2	−2.6	1.9	0.74	1.29	12	−7	16	21	−5
	G3	−0.7	−0.7	0.75	0.48	−11	−19	15	13	4
	G4	−1.1	−2.5	0.74	0.67	−13	2	15	16	3
X = Cl, Z = S	G1	−1.4	−0.8	0.78	0.83	1	−24	15	18	3
	G2	−3.1	2.2	0.72	1.34	4	−8	16	21	−5
	G3	−0.7	−0.1	1.13	0.48	0	−19	16	13	5
	G4	−1.7	0.3	1.06	0.71	2	3	13	13	1
X = Br, Z = S	G1	−1.5	−0.6	0.82	0.84	−1	−24	15	18	4
	G2	−3.2	2.4	0.76	1.35	2	−7	15	20	−4
	G3	−0.7	0.1	1.28	0.56	5	−21	16	14	5
	G4	−1.7	2.6	1.22	0.90	7	1	13	14	−2
X = H, Z = S	G1	−1.9	0.5	0.59	1.28	8	−29	14	22	−6
	G2	−3.3	2.9	0.68	1.61	13	−16	17	24	−11
X = CH_3, Z = S	G1	−1.8	1.6	0.54	1.55	7	−32	12	26	−7
	G2	−3.7	3.8	0.72	1.87	12	−19	17	28	−11

and Z = O, S), and this is larger for **G3** and **G4** in ZCHO···HNO than for that in XCHS···HNO. On the other hand, increase in the s-character percentage of the C1(H2) atom in **G1** and **G2** of XCHO···HNO is smaller than that in XCHS···HNO (X = CH_3, H, F, Cl, and Br). Such an increase is consistent with Bent's rule predicting an increase of the s-character of A-hybrid of the A−H bond when the H atom becomes more electropositive.[56] It is normal that for the blue-shifting hydrogen bond A−H···B, the net charge on A becomes more negative and that on H more positive, leading to an increase in the polarity of the A−H bond. As a matter of fact all the H2 atoms become more positively charged upon complexation as shown in Table 6. The observed gain of positive charge on the H2 atom is ca. 0.012−0.024 au, which will make this hydrogen more attractive to the negatively charged N6 and O5 atoms of HNO and results in the strength of hydrogen-bonded complexes. For the C1 atom, a net gain (0.00−0.0013 au) in electron density is obtained for **G3** and **G4** of FCHZ···HNO (Z = O, S), **G1** and **G2** of XCHO···HNO (X = Cl, Br), and **G1** of BrCHS···HNO, while a net loss (0.001−0.018 au) of electron density is observed for all remaining complexes. This means that there is an increase in the polarization of the C1−H2 bond for the former, while a decrease of this property is observed for the latter as a result of complex formation.

It is interesting that for all complexes, there is a decrease in electron density of all σ^*(C1−H2) orbitals in the range of 0.001−0.007 au. In general, occupation in the σ^*(C1−H2) orbital of XCHO···HNO decreases more strongly than that of XCHS···HNO (cf. Table 6). The decrease in the occupation of the σ^*(C1−H2) orbitals leads to a contraction of the C1−H2 bonds, and subsequently contributes to an increase of its stretching frequency (as compared to the monomer). In addition, an increase in the s-character of the C1(H2) hybrid orbital results in a contraction of the C1−H2 bond. Thus, contraction of the C1−H2 bond length and blue shift of its stretching frequency arise from both a decrease of electron density in the σ^*(C1−H2) orbitals and an increase in the s-character percentage of the C1(H2) center. However, for the different complexes the contributive magnitude of the two factors to the frequency blue shift is not uniform. For instance, the largest decrease of electron density in the σ^*(C1−H2) orbitals causes the strongest blue shift of the C1−H2 bond in XCHO···HNO (X = H, CH_3), although the magnitude of the increase in the s-character of the C1(H2) atom remains small. This suggests that for these complexes, the occupation of the σ^*(C1−H2) orbital is the main factor governing the contraction of C1−H2 bond length and blue shift of its frequency. Likewise, this observation is also verified for **G1** and **G2** of all remaining complexes pairing XCHZ with HNO. However, with a smaller decrease of electron density in the σ^*(C1−H2) orbitals (as compared to that in **G1** and **G2**), it may be noted that the blue shift of the C1−H2 bonds in **G3** and **G4** of XCHZ···HNO is also determined by a significant increase of the s-character of the C1(H2) atom.

Regarding the factors influencing the N6−H7 bond, results recorded in Table 6 show that a significant increase (0.013−0.037 au) in positive charge on the H7 atom appears in all complexes. Simultaneously, the N6 atom is also more negatively charged by ca. 0.0004−0.042 au in all complexes as compared to monomer, except for a slight decrease (0.00−0.003 au) of negative charge on the N6 atom in **G4** of XCHZ···HNO (X = F, Cl, Br and Z = O, S). These results suggest that the polarity of the N6−H7 bond tends to increase in the former and decrease in the latter. Similar to increase in the s-character percentage of the C1(H2) hybrid orbital, a significant increase of this property in the N6(H7) hybrid orbital is equally found, by

0.5−2.1%. The largest increase for the N6(H7) hybrid orbital is obtained in $CH_3CHO\cdots HNO$, and the smallest in $FCHS\cdots HNO$. The magnitude of the s-character of the N6(H7) orbital is quite large in $XCHZ\cdots HNO$ (X = CH_3, H and Z = O, S), while a small increase in s-character percentage of C1(H2) hybrid orbital is detected (cf. above). For each complex, the magnitude of the increase in s-character of N6(H7) is larger for **G1** than for **G3**, and larger for **G2** than for **G4**. This is also in contrast to the variable changes in s-character percentage in the C1(H2) hybrid orbital. Changes in the occupation of the σ^*(N6−H7) orbital also vary due to complexation. The negative value of the $\Delta\sigma^*$(N6−H7) parameters, by an amount of 0.0−0.004 au, for structures such as **G1** and **G2** of $XCHO\cdots HNO$ (X = CH_3, H, F, Cl, and Br), **G3** and **G4** of $XCHO\cdots HNO$ (X = F, Cl), **G1** of $XCHS\cdots HNO$ (X = F, Cl, Br), and **G3** of $XCHS\cdots HNO$ (X = F, Cl), indicates an effective decrease in electron density of the σ^*(N6−H7) orbital following complexation. Therefore, contraction and blue shift of the N6−H7 bond are governed by both factors, namely a decrease in occupation of the σ^*(N6−H7) orbital and an increase in s-character percentage of the N6(H7) hybrid orbital. Accordingly, the largest contraction of the N6−H7 length in $CH_3CHO\cdots HNO$ apparently results from the largest increase in the s-character of the N6(H7) atom and the largest decrease of the σ^*(N6−H7) orbital electron density.

Moderate increase (0.0−0.004 e) in the σ^*(N6−H7) electron density is found in the remaining complexes including **G3** and **G4** of $BrCHO\cdots HNO$, **G2** and **G4** of $ClCHS\cdots HNO$, **G2** of $FCHS\cdots HNO$, **G2**, **G3**, and **G4** of $BrCHS\cdots HNO$, and **G1** and **G2** of $XCHS\cdots HNO$ (X = CH_3, H). Hence, the blue shift of the υ(N6−H7) stretching frequencies in these complexes is basically determined by increase in the s-character percentage of the N6(H7) hybrid orbital, which overcomes the increase in occupation of the σ^*(N6−H7) orbital.

The dual correlations between the changes of the bond length and stretching frequency of the N6−H7 bond with the changes of electron density in the σ^*(N6−H7) orbitals and hybridization in the N6(H7) hybrid orbitals in all examined structures can be expressed in the following equations:

$$\Delta r(\text{N6−H7})\ (\text{Å}) = 0.392\Delta\sigma^*(\text{N6−H7})\ (\text{au}) - 0.002\Delta\%\text{s(N6)} \quad (r = 0.98) \quad (3)$$

$$\Delta\upsilon(\text{N6−H7})\ (\text{cm}^{-1}) = -6790.9\Delta\sigma^*(\text{N6−H7})\ (\text{au}) + 37.7\Delta\%\text{s(N6)} + 13.1 \quad (r = 0.99) \quad (4)$$

Similar dual correlations of these parameters are also obtained for the C1−H2 bonds of the complexes pairing XCHO with HNO:

$$\Delta r(\text{C1−H2})\ (\text{Å}) = 0.5062\Delta\sigma^*(\text{C1−H2})\ (\text{au}) - 0.000.3\Delta\%\text{s(C1)} \quad (r = 0.95) \quad (5)$$

$$\Delta\upsilon(\text{C1−H2})\ (\text{cm}^{-1}) = -6211.1\Delta\sigma^*(\text{C1−H2})\ (\text{au}) + 6.1\Delta\%\text{s(C1)} + 5.7 \quad (r = 0.96) \quad (6)$$

From eqs 3−6, with the much larger slope of $\Delta\sigma^*$(C1−H2) and $\Delta\sigma^*$(N6−H7) parameters with respect to $\Delta\%$s(C1) and $\Delta\%$s(N6), respectively, it is clear that the variations in electron density of the σ^*(N6−H7) and σ^*(C1−H2) orbtials mainly govern the behavior of both C1−H2 and N6−H7 bond lengths and their stretching frequencies upon interaction. To check further the reliability of these correlations, we recalculated the changes of bond length based on eqs 3 and 5, as well as those of stretching frequency based on eqs 4 and 6, employing the respective values for $\Delta\sigma^*$(N6−H7), $\Delta\sigma^*$(C1−H2), $\Delta\%$s(N2), and $\Delta\%$s(C1) as listed in Table 6, and then compared the so-obtained values to the real variations recorded in Tables 1 and 3. A comparison indicates that the correlations are quite reliable as illustrated in Figure 3 in the Supporting Information.

4. Concluding Remarks

In the present theoretical study on the complexes derived from interaction between simple derivatives of formaldehyde and thioformaldehyde with the HNO molecule, 32 local minima were identified on the corresponding potential energy surfaces. Interaction of CH_3CHO with HNO was found to lead to the most stable complex, whereas the pair of FCHS and HNO results in the least stable complex. All the C−H and N−H bonds are characterized by a shortening in bond length and a blue shift in frequency upon complexation. In general, the corresponding decrease in infrared intensity is observed for the C−H and N−H bonds in all of the complexes, except for an increase of infrared intensity in some complexes of ClCHS and BrCHS with HNO. The magnitude of the deviations observed depends on the polarity of the C−H bond in isolated monomers. Changes in the N−H bond characteristics arise from an intrinsic behavior of the HNO isolated monomer. Highly linear correlations between the changes of stretching frequency and bond length of both N−H and C−H bonds in all complexes were also evaluated. It is remarkable that the changes in the N−H bond length and stretching frequency can be approached as a dual function of both occupations in the original σ^*(N−H) orbitals and s-character of the N hybrid orbitals. The other dual correlations are also predicted for the C1−H2 bonds in the complexes pairing XCHO with HNO.

Acknowledgment. We are indebted the K.U.Leuven Research Council (GOA and IDO programs) and the Vietnam National Foundation for Science and Technology Development (NAFOSTED) for financial support. N.T.T thanks Professor Thérèse Zeegers-Huyskens for valuable discussion.

Supporting Information Available: Cartesian coordinates of all complexes considered and changes in geometrical parameters compared to monomer. This material is available free of charge via the Internet at http://pubs.acs.org.

References and Notes

(1) Desiraju, G. R.; Steiner, T. *The Weak Hydrogen Bond in Structural Chemistry and Biology*; Oxford University Press: New York, 1999.
(2) Grabowski, S. J. *Hydrogen bonding-New Insights*; Springer: Dordrecht, The Netherlands, 2006.
(3) Buckingham, A. D.; Fowler, P.; Hutson, J. M. *Chem. Rev.* **1988**, *88*, 963.
(4) Meyer, E. A.; Castellano, R. K.; Diederich, F. *Angrew Chem., Int. Ed.* **2003**, *42*, 1210.
(5) Scheiner, S. *Hydrogen Bonding*; Oxford University Press: New York, 1997.
(6) Soriano, A.; Castillo, R.; Christov, C.; Andres, J.; Moliner, V.; Tunon, I. *Biochemistry* **2006**, *45*, 14917.
(7) Lewinski, J.; Zachara, J.; Justyniak, J.; Dranka, M. *Coord. Chem. Rev.* **2005**, *249*, 1185.
(8) Barbolina, M. V.; Phillips, R. S.; Gollnick, P. D.; Faleev, N. G.; Demidkina, T. V. *Protein Eng.* **2000**, *13*, 207.
(9) Hobza, P.; Spirko, V. *Phys. Chem. Chem. Phys.* **2003**, *5*, 1290.
(10) Kryachko, E. S.; Zeegers-Huyskens, T. *J. Phys. Chem. A* **2001**, *105*, 7118.
(11) Gu, Y.; Kar, T.; Scheiner, S. *J. Am. Chem. Soc.* **1999**, *121*, 9411.
(12) Hobza, P. *Phys. Chem. Chem. Phys.* **2001**, *3*, 2555.
(13) Alabugin, I. V.; Manoharan, M.; Peabody, S.; Weinhold, F. *J. Am. Chem. Soc.* **2003**, *125*, 5973.

(14) Joseph, J.; Jemmis, E. D. *J. Am. Chem. Soc.* **2007**, *129*, 4620.
(15) Hermansson, W. *J. Phys. Chem. A* **2002**, *106*, 4695.
(16) Jeffery, P. G. A. *An Introduction to Hydrogen Bonding*; Oxford University Press: New York, 1997.
(17) Reimann, B.; Buchhold, K.; Vaupel, S.; Brutschy, B.; Halvas, Z.; Spiro, V.; Hobza, P. *J. Phys. Chem. A* **2001**, *105*, 5560.
(18) Hobza, P.; Spirko, V.; Havlas, Z.; Buchhold, K.; Reimann, B.; Barth, H. D.; Brutschy, B. *Chem. Phys. Lett.* **1999**, *299*, 180.
(19) (a) Hobza, P.; Havlas, Z. *Chem. Rev.* **2000**, *100*, 4253. (b) Hobza, P.; Havlas, Z. *Theor. Chem. Acc.* **2002**, *108*, 325.
(20) Karpfen, A.; Kryachko, E. S. *J. Phys. Chem. A* **2003**, *107*, 9724.
(21) Li, X. S.; Liu, L.; Schlegel, H. B. *J. Am. Chem. Soc.* **2002**, *124*, 9639.
(22) Scheiner, S.; Kar, T. *J. Phys. Chem. A* **2002**, *106*, 1784.
(23) Pejob, L.; Hermansson, K. *J. Chem. Phys.* **2003**, *119*, 313.
(24) Qian, W.; Krimm, S. *J. Phys. Chem. A* **2005**, *109*, 5608.
(25) Scheiner, S.; Grabowski, S. J.; Ka, T. *J. Phys. Chem. A* **2001**, *105*, 10607.
(26) Masunov, A.; Dannenberg, J. J.; Contreras, R. H. *J. Phys. Chem. A* **2001**, *105*, 4737.
(27) Li, A. Y. *J. Phys. Chem. A* **2006**, *110*, 10805.
(28) Hobza, P. *Int. J. Quatum Chem.* **2002**, *90*, 1071.
(29) Liu, Y.; Liu, W.; Yang, Y.; Liu, J. *Int. J. Quantum Chem.* **2006**, *106*, 2122.
(30) Liu, Y.; Liu, W.; Li, H.; Liu, J.; Yang, Y. *J. Phys. Chem. A* **2006**, *110*, 11760.
(31) Yang, Y.; Zhang, J. W.; Gao, X. M. *Int. J. Quantum Chem.* **2006**, *106*, 1199.
(32) Liu, Y.; Liu, W.; Li, H.; Yang, Y.; Cheng, S. *Int. J. Quantum Chem.* **2007**, *107*, 396.
(33) Solimannejad, M.; Scheiner, S. *J. Phys. Chem. A* **2008**, *112*, 4120.
(34) Solimannejad, M.; Scheiner, S. *J. Phys.Chem. A* **2007**, *111*, 4431.
(35) Yang, Y.; Zhang, W. *THEOCHEM.* **2007**, *814*, 113.
(36) Trung, N. T.; Hue, T. T.; Nguyen, M. T.; Zeegers-Huyskens, Th. *Phys. Chem. Chem. Phys.* **2008**, *10*, 5105.
(37) Liu, Y. *Int. J. Quantum Chem.* **2008**, *108*, 1123.
(38) Trung, N. T.; Hue, T. T.; Nguyen, M. T. *Phys. Chem. Chem. Phys.* **2009**, *11*, 926.
(39) Bunte, S. W.; Rice, B. M.; Chalalowski, C. F. *J. Phys. Chem. A* **1997**, *101*, 9430.
(40) Liu, Y.; Liu, W. Q.; Li, H. Y.; Yang, Y.; Cheng, S. *Chin. J. Chem.* **2007**, *25*, 44.
(41) Karpfen, A.; Kryachko, E. *J. Phys. Chem. A* **2005**, *109*, 8930.
(42) Karpfen, A.; Krychachko, E. *J. Phys. Chem. A* **2007**, *111*, 8177.
(43) Dunning, T. H. *J. Chem. Phys.* **1989**, *90*, 1007.
(44) Li, Q.; An, X.; Luan, F.; Li, W.; Cheng, J. *J. Phys. Chem. A* **2008**, *112*, 3985.
(45) Ringer, A. L.; Figgs, M. S.; Sinnokrot, M. O.; Sherrill, C. D. *J. Phys. Chem. A* **2006**, *110*, 10822.
(46) Tsuzukim, S.; Fuijii, A. *Phys. Chem. Chem. Phys.* **2008**, *10*, 2584.
(47) Boys, S. F.; Bernadi, F. *Mol. Phys.* **1970**, *19*, 553.
(48) Frisch, M. J.; Trucks, G. W.; Schlegel, H. B.; Scuseria, G. E.; Robb, M. A.; Cheeseman, J. R. ; Montgomery, J. A., Jr.; Vreven, T.; Kudin, K. N.; Burant, J. C.; Millam, J. M.; Iyengar, S. S.; Tomasi, J.; Barone, V.; Mennucci, B.; Cossi, M.; Scalmani, G.; Rega, N.; Petersson, G. A.; Nakatsuji, H.; Hada, M.; Ehara, M.; Toyota, K.; Fukuda, R.; Hasegawa, J.; Ishida, M.; Nakajima, T.; Honda, Y.; Kitao, O.; Nakai, H.; Klene, M.; Li, X.; Knox, J. E.; Hratchian, H. P.; Cross, J. B.; Adamo, C.; Jaramillo, J.; Gomperts, R.; Stratmann, R. E.; Yazyev, O.; Austin, A. J.; Cammi, R.; Pomelli, C.; Ochterski, J. W.; Ayala, P. Y.; Morokuma, K.; Voth, G. A.; Salvador, P.; Dannenberg, J. J.; Zakrzewski, V. G.; Dapprich, S.; Daniels, A. D.; Strain, M. C.; Farkas, O.; Malick, D. K.; Rabuck, A. D.; Raghavachari, K.; Foresman, J. B.; Ortiz, J. V.; Cui, Q.; Baboul, A. G.; Clifford, S.; Cioslowski, J.; Stefanov, B. B.; Liu, G.; Liashenko, A.; Piskorz, P.; Komaromi, I.; Martin, R. L.; Fox, D. J.; Keith, T.; Al-Laham, M. A.; Peng, C. Y.; Nanayakkara, A.; Challacombe, M.; Gill, P. M. W.; Johnson, B.; Chen, W.; Wong, M. W.; Gonzalez, C.; Pople, J. A. *Gaussian 03*, revision D.02; Gaussian: Wallingford, CT, 2004.
(49) *AIM 2000* designed by Friedrich Biegler-König, University of Applied Sciences, Bielefeld, Germany.
(50) Bader, W. J. F. *Chem. Rev.* **1991**, *91*, 893.
(51) Popelier, P. *Atoms in Molecules*; Pearson Education Ltd.: Essex, U.K., 2000.
(52) Glendening, E. D.; Baderhoop, J. K.; Read, A. E.; Carpenter, J. E.; Bohmann, J, A.; Weinhold, F. *GenNBO 5.0G*; Theoretical Chemistry Institue, University of Wisconsin, Madison, WI, 1996−2001.
(53) Keefe, C. D.; Isenor, M. *J. Phys. Chem. A* **2008**, *112*, 3129.
(54) NIST webpage: http://webbook.nist.gov/chemistry.
(55) Koch, U.; Popelier, P. L. A. *J. Phys. Chem.* **1995**, *99*, 9747.
(56) Bent, H. A. *Chem. Rev.* **1961**, *61*, 275.

JP810826Z